Power Spectral Density Model for Pedestrian Walking Load

Jun Chen[1, 2, *], Jinping Wang[1], James M.W. Brownjohn[3]

[1] *College of Civil Engineering, Tongji University, Shanghai, P. R. China*

[2] *State Key Laboratory of Disaster Reduction in Civil Engineering, Tongji University, P. R. China*

[3] *Vibration Engineering Section, University of Exeter, Exeter EX4 4QF, United Kingdom*

Abstract: Intensive vibrations may occur in slender structures like footbridges and long-span floors due to movement of pedestrians. Problems are usually treated in time domain as Fourier series models of the forcing function, but most methods have disadvantages of neglecting the stochastic character of human walking, being computationally inefficient for random vibration analysis and overestimating responses in the case of resonance. Meanwhile, frequency domain models of other types of structural loading are efficient while being a more acceptable approach widely adopted for dealing with stochastic response problems. Hence, an experiment-based power spectral density (PSD) model normalized to walking frequency and order of harmonic is proposed. To construct this model, 1528 individual walking load time histories were collected from an experiment on a rigid floor. These records were then linked to obtain a smaller number of longer samples for a good frequency resolution in spectral analysis. Using the linked samples and for frequency normalized to mean walking frequency, PSD models for the range 1 ± 0.05 for the harmonic and the sub-harmonic are suggested as Gaussian mixture with eight model parameters. Via the stationary and non-stationary stochastic vibration theory, the proposed model is used to predict the structural response in terms of root-mean-square and peak of acceleration. The framework is finally tested via field measurements demonstrating applicability in practical design work.

* Corresponding Author: cejchen@tongji.edu.cn

Keywords: Walking load; Power spectral density; Stochastic vibrations; Vibration serviceability.

Introduction

Due to the significant advance and wide application of light-weight and high-strength construction materials, structures like long-span floors and footbridges are even more distinctly characterized with lightness and slenderness. Accounting for the low natural frequency and damping ratio of this type of slender structure, when human activities like walking and jumping take place, excessive unpleasant vibration might appear. In history, many buildings and bridges have experienced this human-induced vibration problem, with occasional but rare tragic consequences. The most infamous case is the Millennium Bridge in London which was caused to vibrate dramatically due to crowd loading (Dallard et al. 2001). In 2013, a pedestrian bridge in Jiangxi Province, China collapsed when a group of tourists crowded into the bridge, causing some people to fall into the water. To avoid such occurrences, a better understanding of the human-induced load on such structures is in great demand.

Numerous researchers have studied this field: Blanchard et al. (1977), Bachmann and Ammann (1987), Rainer et al. (1988), Allen and Murray (1993), Petersen (1996), Kerr (1998), Yoneda (2002) and Chen et al. (2014) have put forward deterministic walking load models in Fourier series. These previous researches mainly focused on dynamic load factors (DLF), coefficients for the deterministic models of walking load in time domain. However, such time-domain models for walking are based on an assumption that both human feet produce exactly the same force and that the force is periodic. In fact, human walking load is a kind of stochastic load by nature because people cannot maintain identical amplitude and duration in each walking step. The proposed models neglect the inter-subject variability (e.g. walking frequency, velocity, force amplitude, and body weight differing between humans) and the intra-subject variability (e.g. the inability of humans to repeat the same force in each step) in the walking process (Živanović et al. 2007). Moreover, though simple in concept and application, deterministic models can overestimate structural response in resonance, especially when resonant with higher orders of harmonics of walking load, as pointed out by Brownjohn et al. (2004) for walking load, and by Racic and Pavic (2010) for jumping load. This is owing to the energy leakage around each harmonic center frequency in real walking, instead of the perfect concentration of energy in deterministic models. Furthermore, the higher the harmonic, the greater the spread of energy. This phenomenon is a result of the stochastic nature of human walking as mentioned.

Probabilistic models, which take account of the randomness, have then been proposed. In time domain, such models have been suggested by Živanović et al. (2007, 2015) and Racic and Brownjohn (2010). The probabilistic models in time domain are quite complicated for stochastic problem analysis, requiring time history calculation and Monte Carlo simulation, which is time-consuming particularly for complex structures (Živanović et al. 2010, Piccardo & Tubino 2012, Caprani 2014). With the help of random vibration theory, load models in frequency domain are relatively easy to use in obtaining the structural response and are more acceptable and widely adopted in dealing with stochastic problems in earthquake and wind engineering (Haselton et al. 2011, Huang et al. 2015). The theories of stationary and non-stationary random processes for application to vibration serviceability appeared earliest in the 1980s (Ohlsson 1982) and later, Brownjohn et al. (2004) first proposed a spectral model based on experimental data from three test subjects when determining the model parameters. The model was presented in the form of Fourier amplitude spectra, which was not scaled to the walking frequency and order of harmonic. Thus, parameters of the first six harmonics in the spectra were identified separately by curve fitting. Drawbacks of this model are that merely three test subjects were involved in the experiment which is not enough for describing inter-subject variability; the spectrum neglects the sub-harmonics which is distinct particularly for the fundamental; the spectrum is only suggested around a certain frequency range of each harmonic and finally energy for higher harmonics presents noticeable overlap in the spectrum. Thereafter, Caprani (2014) took advantage of the previous model (Brownjohn et al. 2004) by digitizing their experimental data to provide a new DLF spectral model, which solves the overlap problem but still has the similar deficiency of limited records. Piccardo and Tubino (2012) and Ferrarotti and Tubino (2016) suggested models for crowd load with non-dimensional parameters derived from the Fourier series walking load function, and the final model considers only the first harmonic. Li et al. (2010) studied the complex crowd-footbridge resonant vibration mechanism with the random vibration approach. Krenk (2012) developed a spectral model with respect to bandwidth of pedestrian load and a compact explicit formula to estimate the structural response. Looking through all these models, large volumes of testing data is prerequisite to represent the randomness of walking load and thus to develop a more accurate experimental spectral model. In addition, applying parallels to the approach for modelling random wind gust loading, the spectral model is better presented in a non-dimensional form, as employed in this research. Thus, a unified function can be adopted to model all the main and sub harmonics.

In this paper, an experiment to collect walking record was conducted, serving as the data source for power spectral density (PSD) modelling. The PSD model is proposed with a special linking method to obtain samples with longer duration, and the model parameters are determined accordingly. To predict structural response, including root-mean-square of acceleration for continuous vibrations as well as the peak acceleration, a methodology making use of stochastic vibration theory is introduced. Field verifications of this methodology on a floor model in the lab and an as-built floor in a railway station were carried out via a comparison of calculated and experimental result. Some limitations and further development of the proposed model are also discussed in the end.

Experiments for collecting walking load samples

A large number of individual walking load data is necessary to develop a PSD model for a stochastic dynamic excitation, and force plates are commonly adopted in walking load measurement. The force plate can only record a single footfall trace (SFT) due to its relatively small size and fixed installation position.

The SFT records are too short, typically less than one second, for spectral property investigation. Although an instrumented treadmill can be used to measure continuous walking load forces (Brownjohn et al. 2004), there are reservations about potential influence of the predefined treadmill belt speed on the test subject's gait (thus variability of walking force). To tackle this problem, a novel wireless insole pressure system (Pedar-x, Germany) was used to measure the continuous walking load time history. While a person was walking, steps were recorded at sampling frequency of 100 Hz with instrumented insoles in the subject's shoes. The Pedar system recorded the pressure distribution under the foot sole using one hundred micro pressure sensors and transmitted the records to data acquisition center (a laptop) wirelessly via Bluetooth technology (Fig. 1). On the laptop, the analysis software Novel helped to collect and present the pressure data, and provided the vertical force and the center of pressure of each foot estimated by integrating all the pressures. The Pedar system has been widely used in gait and biomechanical studies and its measurement accuracy is well acknowledged (Lee and Hong 2005, Forner Cordero et al. 2004). Nevertheless, the Pedar system used in this study was calibrated by comparing its measurements with those from force plate. Moreover, for each test case the standard test protocol was strictly followed to reduce pressure sensor's zeroing effect. As an example, Fig. 2a show time histories of the measured walking load of the left, right foot and their summation, the Fourier amplitude spectrum of the total force is shown in Fig. 2b.

Fig.1. Test subject with Pedar insole system in the experiment

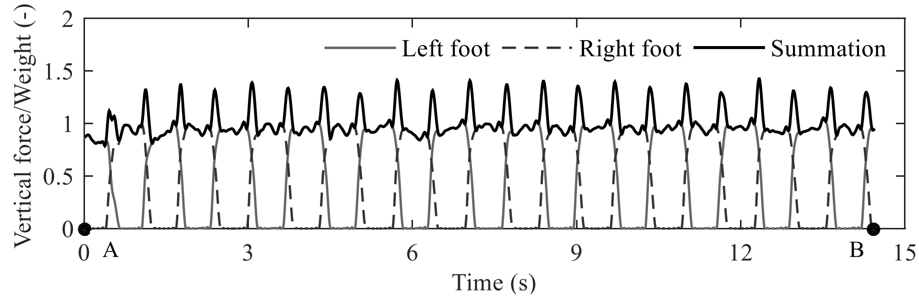

(a) Normalized vertical force of left, right foot and their summation

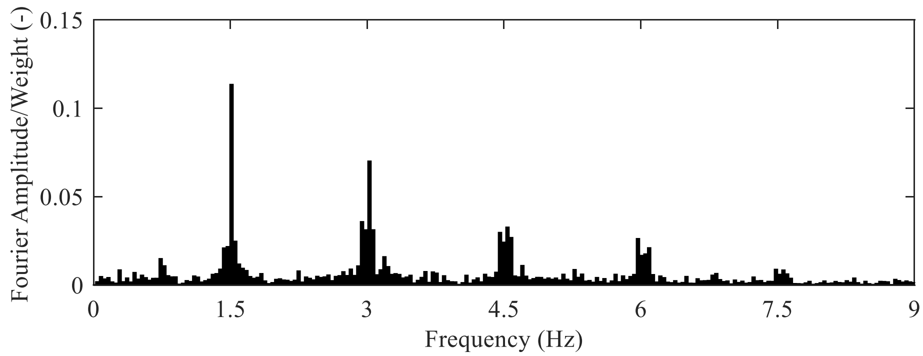

(b) Fourier amplitude spectrum of total force

Fig. 2. Typical testing samples at f_p = 1.50 Hz

Fifty-six test subjects participated in the experiment. Statistical features of all the test subjects are shown in Table 1. Each test subject performed 11 test cases, including eight cases with fixed walking frequencies f_p (1.50, 1.65, 1.75, 1.80, 1.95, 2.00, 2.10, and 2.25 Hz) and three free-walking cases (self-controlled slow, normal, and fast rates). The eight fixed walking frequencies cover the range for a test subject to maintain normal gait. Each frequency was instructed by a metronome, e.g. 90 beats per minute for 1.5 Hz. For each case, each test subject walked along a 40 m long path on a rigid floor and repeated three times. The test protocol satisfied the requirements by Tongji Medical Ethics Committee. In total, 1528 continuous walking loads were collected from the experiment.

Table 1. Statistics of age, body mass and height of the test subjects

Gender	No.	Age (Year)			Body Mass (kg)			Height (cm)		
		Mean	Std.	Range	Mean	Std.	Range	Mean	Std.	Range
Male	39	24.0	2.52	20-29	68.3	15.00	49.8-95.1	174.6	47.58	156-197
Female	17	23.7	6.37		60.3	4.98		162.6	21.28	

Power spectral density model

This section describes the development of a PSD model for individual walking load that is treated as a narrowband stationary stochastic process in time domain. The same assumption was adopted in the work of Brownjohn et al. (2004) and Eriksson (1994). A mathematical expression for PSD is first proposed whose parameters are identified from the experiment records.

Basic equations

The PSD of a stationary stochastic process $x(t)$ is defined as (Wirsching and Paez 2006):

$$S_X(f) = \lim_{T\to\infty} \frac{1}{T} E\left[\left|X(f,T)\right|^2\right] \quad -\infty < f < \infty \tag{1}$$

where $E[\square]$ is the ensemble average, $|\square|$ means the absolute value, f is frequency in Hertz, T and $X(f,\ T)$ are duration and Fourier transform of $x(t)$

$$X(f,T) = \int_{-\infty}^{+\infty} x(t) e^{-\mathrm{i}2\pi ft} \mathrm{d}t \tag{2}$$

To avoid use of negative frequency, single-sided PSD is defined as

$$G_X(f) = \begin{cases} 2S_X(f) & f > 0 \\ S_X(f) & f = 0 \\ 0 & f < 0 \end{cases} \tag{3}$$

Construction of new samples

Generally, in practical work, with limited number of samples of limited durations, PSD is usually calculated through the periodogram method: PSD of each measured record, i.e., sample realizations of the stochastic process, can be obtained as sample PSDs and their average is taken as the PSD of the stochastic dynamic excitation. Equation (2) indicates that in theory a sample with infinite duration is required for PSD calculation. Moreover, because the walking load is a near-periodic random process, its PSD curve is expected to have a sharp change at each peak's adjacent region (Brownjohn et al. 2004). A fine frequency resolution is therefore imperative for describing local features around each PSD's peak. The duration of the original recorded sample is typically 20-36 s leading to a frequency resolution up to 0.05 Hz, which is very poor for a near-periodic process. As an example, Fig. 3 shows the PSD, around the first four harmonics, of a 1.5 Hz walking test sample whose actual frequency resolution is df = 0.0325 Hz.

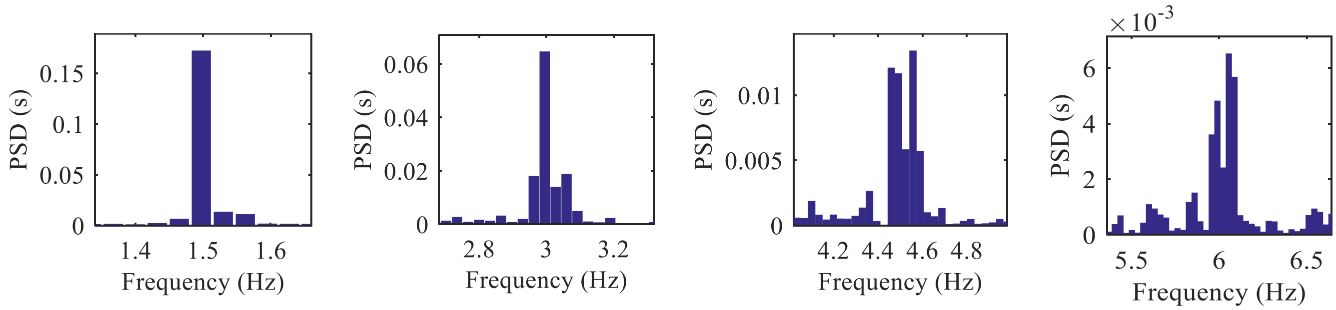

(a) The 1st harmonic (b) The 2nd harmonic (c) The 3rd harmonic (d) The 4th harmonic

Fig. 3. The PSD of a walking load sample normalized to body weight at f_p = 1.50 Hz (df = 0.0325 Hz)

To tackle the resolution problem, new samples of longer duration are constructed using original records by the following steps. Each original record, summation of records of both feet, has been firstly normalized by the test subject's static body weight. The normalized record was then truncated from one foot's initial contact with the ground of the first footfall (i.e., point A in Fig. 2a) to the same foot's final contact with the ground of the last footfall (i.e., point B in Fig. 2a) in the time history. The dominant frequency of each truncated record of around 20 s was identified from its Fourier amplitude spectrum as shown in Fig. 2b. Those records whose dominant frequencies are not in the range $f_p \pm 0.025$ Hz were taken as unqualified ones and excluded from further analysis, where f_p is the specified walking frequency in the test. All the qualified records from the same test case (i.e. the same prompted frequency f_p) can be assumed as samples of the same random stationary process. They were then connected end-to-end to form a new sample. The durations of the constructed new samples are 3200, 2600, 4000, 2200, 2000, 3000, 1800, and 1800 seconds for walking frequencies 1.50, 1.65, 1.75, 1.80, 1.95, 2.00, 2.10, and 2.25 Hz, respectively. Run tests (Bendat and Piersol 2000) were conducted on all the new samples, and they all passed the test with a significance level of 0.05 and a test segment number of 50, indicating that the stationarity assumption is tenable for all the constructed new samples.

Power spectral density of new sample

To determine the PSD of the new samples, Welch method (Welch 1967) with Hanning window (Grandke 1983) was used: each new sample was divided into several segments (around 40-70 segements) with fifty percent overlap. Duration of each segment was so selected that it was long enough for a good frequency resolution should be N (integer) times over the test pacing period $T_p = 1/f_p$. The second criterion was adopted to avoid numerical leakage in Fourier analysis and for walking frequency normalization later. Figure 4 shows the so-obtained PSD $G_{X_w}(f)$ (where X_w denotes the walking load) for 1.50 and 2.25 Hz test walking frequency cases, the frequency resolution in both cases is $df = f_p/100$, i.e. the duration of each segment is 100 times T_p.

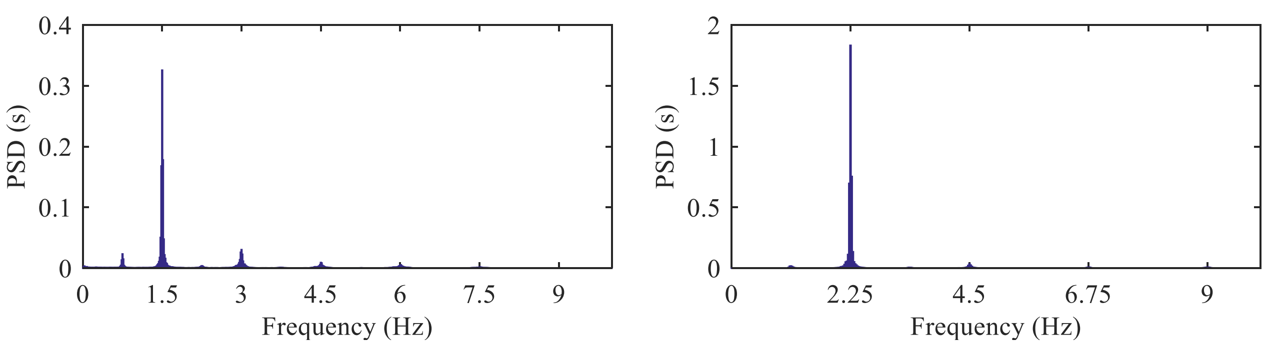

(a) f_p = 1.50 Hz (b) f_p = 2.25 Hz,

Fig. 4. The PSD $G_{X_{\mathrm{w}}}(f)$ of the new samples normalized to body weight with d$f = f_{\mathrm{p}}/100$

Note from Fig. 4 that the walking load energy mainly distributes around the first several harmonics (i.e., frequencies at 1, 2, 3, and 4 times of f_{p}) and sub-harmonics (i.e., frequencies at 0.5, 1.5, 2.5, and 3.5 times of f_{p}). The distribution range becomes more pronounced for higher harmonics. This phenomenon justifies once again the narrowband stochastic process assumption for walking load. Based on the above observation, spectral modelling is focused mainly on a range of each harmonic or sub-harmonic of the PSD curve, which is [$0.95nf_{\mathrm{p}}$, $1.05nf_{\mathrm{p}}$] where n is the order of harmonic or sub-harmonic. The energy, in other words, the enclosed area of PSD curve within the distribution frequency range, for each harmonic (sub-harmonic) can be calculated as

$$S_n = \int_{0.95nf_{\mathrm{p}}}^{1.05nf_{\mathrm{p}}} G_{X_{\mathrm{w}}}(f)\,\mathrm{d}f \quad (4)$$

The calculation results for the first four harmonics, i.e., n = 1, 2, 3, and 4, and the first four sub-harmonics, i.e., n = 0.5, 1.5, 2.5, and 3.5, are shown in Table 2. To account for the load energy between each harmonic later, total energy of the PSD curve in the whole frequency range (0-50 Hz) was also calculated and given in Table 2 as S_0.

$$S_0 = \int_{0}^{50} G_{X_{\mathrm{w}}}(f)\,\mathrm{d}f \quad (5)$$

Table 2. PSD energy normalized to body weight of every harmonic S_n (10^{-3})

f_p (Hz)	Harmonics				Sub-harmonics				Total	$\Sigma S_{sub} / \Sigma S_n$* (-)	$\Sigma S_n / S_0$ (-)
	S_1	S_2	S_3	S_4	$S_{0.5}$	$S_{1.5}$	$S_{2.5}$	$S_{3.5}$	S_0		
1.50	12.72	2.48	1.02	0.86	0.87	0.35	0.21	0.15	22.61	8.47%	83%
1.65	21.05	1.91	0.85	0.92	0.89	0.44	0.20	0.13	30.73	6.29%	86%
1.75	28.76	1.48	0.90	1.03	1.12	0.51	0.21	0.18	40.03	5.91%	85%
1.80	33.52	1.34	0.85	1.05	0.94	0.49	0.16	0.09	43.38	4.37%	89%
1.95	52.63	2.33	0.76	1.19	1.47	0.75	0.22	0.13	63.47	4.32%	94%
2.00	56.25	2.30	0.83	1.29	1.21	0.70	0.22	0.13	66.92	3.59%	94%
2.10	62.73	2.84	0.80	1.22	1.17	0.67	0.20	0.12	74.17	3.10%	94%
2.25	84.76	3.33	1.05	1.46	1.20	0.75	0.23	0.14	99.09	2.50%	94%

* $\Sigma S_{sub} = S_{0.5} + S_{1.5} + S_{2.5} + S_{3.5}$, $\Sigma S_n = \Sigma S_{sub} + S_1 + S_2 + S_3 + S_4$.

Non-dimensional experimental PSD model

Note from Table 2 that the first four harmonics and sub-harmonics contain most of the walking load energy, so rationally, they are considered in the following modelling process. First, the PSD values within [$0.95nf_p$, $1.05nf_p$] of each curve are divided by its corresponding S_n, i.e., the energy for each harmonic as shown in Table 2, thus making the enclosed area of each curve to be unity. Second, the frequency axis was divided by walking frequency f_p and the amplitude axis multiplied f_p, leading to the eight frequency-normalized PSD curves (four harmonics and four sub-harmonics) as shown in Fig. 5 together with an average curve. Third, all the eight average PSD curves in Fig. 5 were normalized to their corresponding order of harmonic (or sub-harmonic). This was done by normalizing the frequency axis by n and multiplying the amplitude axis by n. The normalized curves are shown in Fig. 6a for harmonic case and Fig. 6b for sub-harmonic case.

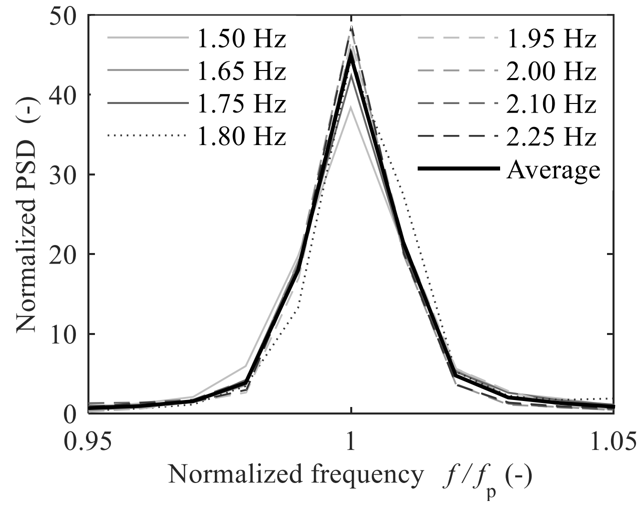

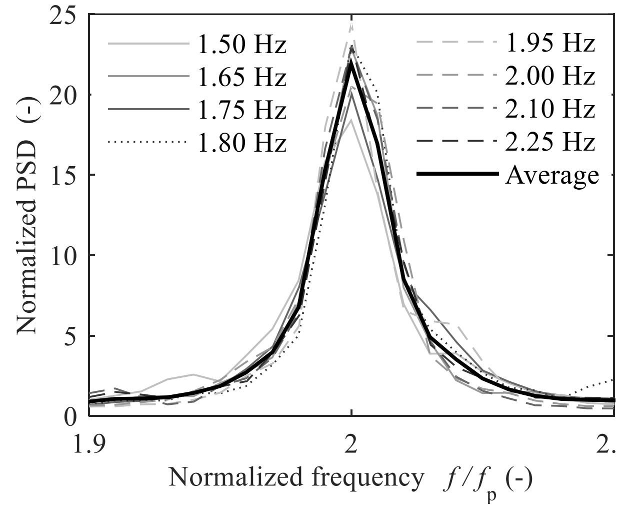

(a) The 1st harmonic

(b) The 2nd harmonic

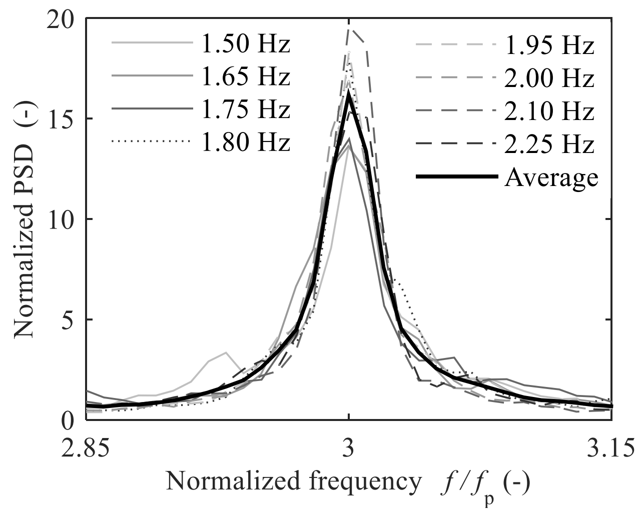

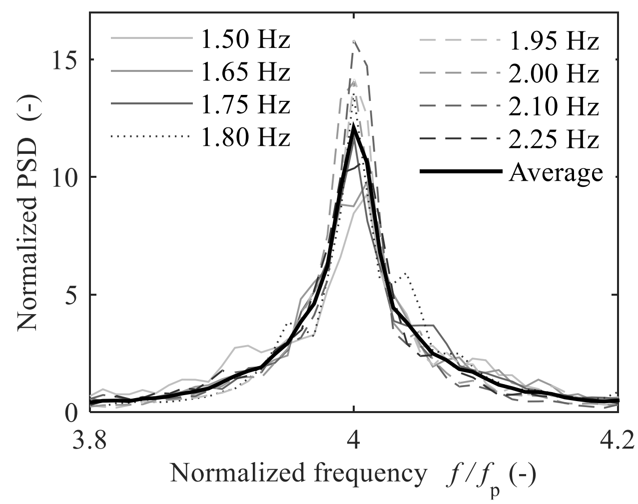

(c) The 3rd harmonic

(d) The 4th harmonic

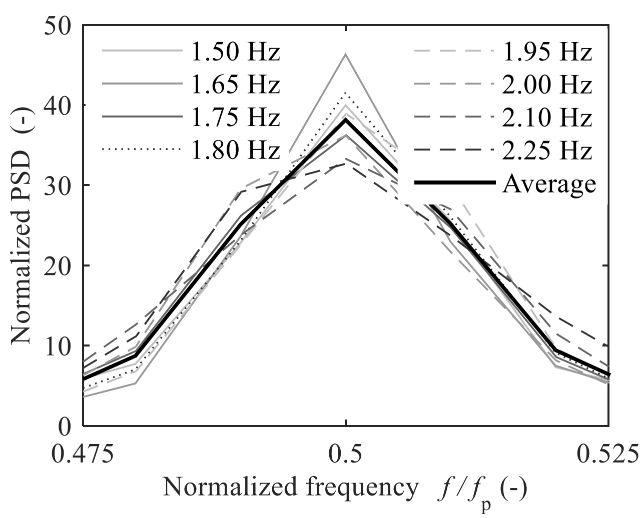

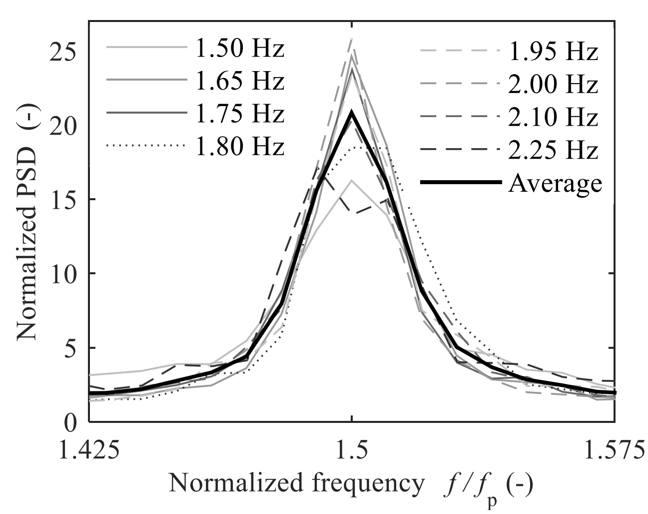

(e) The 1st sub-harmonic

(f) The 2nd sub-harmonic

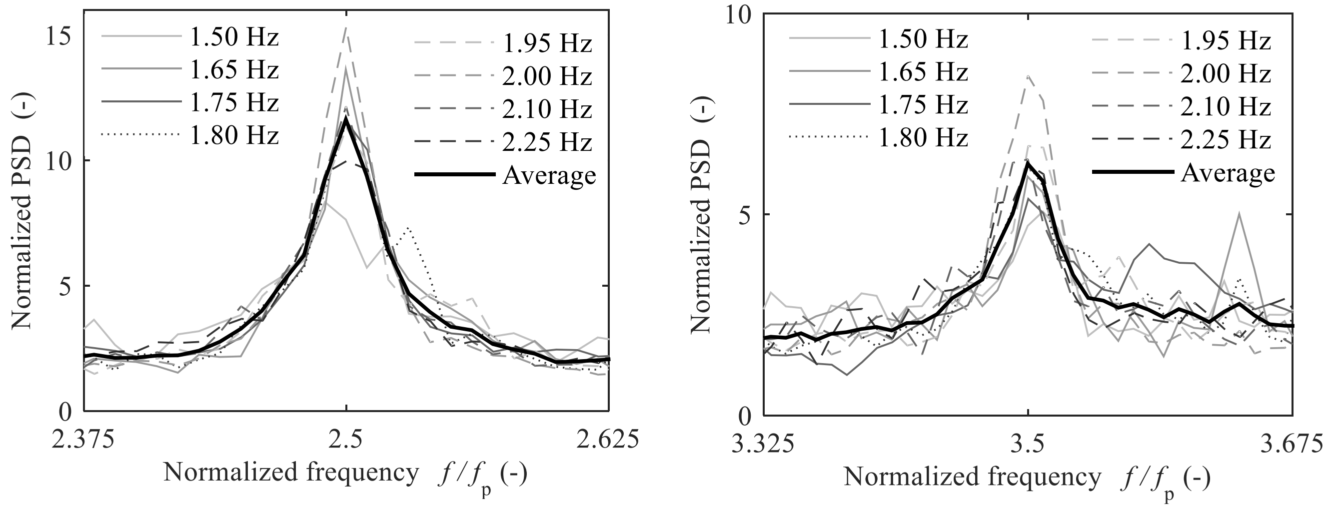

(g) The 3rd sub-harmonic (h) The 4th sub-harmonic

Fig. 5. Superimposed PSD of the new samples and their average

After order-normalization, for different harmonics, the frequency spacing (i.e., d*f*/*n*) is not the same, as demonstrated by the symbol of each curve in Fig. 6. Thus, all the curves were resampled to the same length and their average, which was weighted with $E(S_n)$, i.e., mean of S_n of the eight walking frequencies corresponding to each harmonic, was calculated and plotted in Fig. 6.

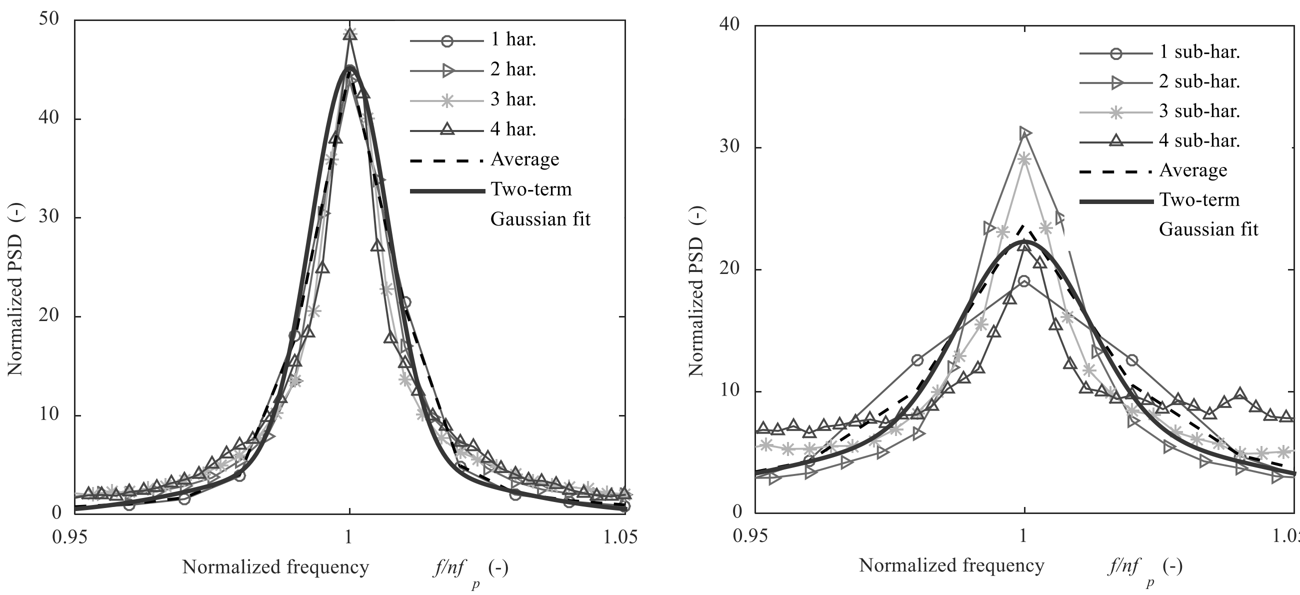

(a) Harmonic (b) Sub-harmonic

Fig. 6. Normalized PSDs of four harmonics (sub-harmonics), the average and the two-term Gaussian fit

Mathematical expression for PSD of walking load

After all the above operations, i.e. normalization of area, frequency, order and taking average, a unified non-dimensional PSD model can then be developed based on results in Fig. 6. Notice the symmetrical bell-shape of the average curve in Fig. 6 and by trial-and-error procedure, a Gaussian mixture for the PSD of walking load at any given walking frequency f_{p} within [1.5, 2.25] Hz were given as :

$$\begin{cases} G_n(f) = \dfrac{\beta S_n}{n f_{\mathrm{p}}} \left\{ A_1 \exp\left[-\left(\dfrac{\bar{f}-1}{\sigma_1} \right)^2 \right] + A_2 \exp\left[-\left(\dfrac{\bar{f}-1}{\sigma_2} \right)^2 \right] \right\}, & f \in \left[0.95 n f_{\mathrm{p}},\ 1.05 n f_{\mathrm{p}} \right] \\ G_n(f) \equiv 0\ , & \text{otherwise} \end{cases} \tag{6}$$

where $G_n(f)$ (unit in second) is the PSD of each harmonic for given walking frequency f_{p}, normalized frequency $\bar{f} = f/(n f_{\mathrm{p}})$ (n = 0.5, 1, 1.5, 2, 2.5, 3, 3.5, and 4), f (unit in Hz) is frequency variable, β (dimensionless) is an energy compensation factor, S_n (unit in second) is the energy of each considered harmonic. Parameters in the model, i.e., A_1, σ_1, A_2, and σ_2 (all dimensionless), were determined by fitting Eq. (6) to the two average curves in Figs. 6a and 6b, and the results are shown in Table 3. Considering the numerical error of curve-fitting, the fitted parameters A_1 and A_2 were scaled by a factor, which is around 1 $\pm$ 0.02, to make sure the area enclosed by the normalized PSD function (i.e., right side of Eq.(6)) is exactly unity.

Table 3. Parameters fitting Eq.(6) of normalized Gaussian fitting PSD

Parameter	A_1	σ_1	A_2	σ_2
Harmonic	40.094	0.0100	5.063	0.034
Sub-harmonic	15.771	0.017	6.515	0.060

To calculate PSD for walking frequency other than that used in the experiment, S_n in Eq. (6) can be obtained through Eq. (7) which is fitted by the experiment results of S_n in Table 2, and the fitting results are summarized in Table 4.

$$S_n = af_\mathrm{p}^3 + bf_\mathrm{p}^2 + cf_\mathrm{p} + d, \quad f_\mathrm{p} \in [1.5,\ 2.25]\ \mathrm{Hz} \tag{7}$$

where n = 0, 0.5, 1, 1.5, 2, 2.5, 3, 3.5, and 4.

Table 4. Parameters for the PSD energy

Para.	Harmonic				Sub-harmonic				Total
	S_1	S_2	S_3	S_4	$S_{0.5}$	$S_{1.5}$	$S_{2.5}$	$S_{3.5}$	S_0
a	-0.1383	-0.0082	0.0029	-0.0016	0.0011	-0.0017	0.0009	0.0015	-0.0821
b	0.7937	0.0557	-0.0144	0.0089	-0.0052	0.0089	-0.0047	-0.0080	0.4952
c	-1.4124	-0.1193	0.0229	-0.0158	0.0086	-0.0153	0.0081	0.0144	-0.8875
d	0.8122	0.0838	-0.0107	0.0099	-0.0039	0.0088	-0.0044	-0.0083	0.5169

The total energy enclosed by PSD curve is crucial for determining response of a structure subjected to the stochastic excitation. Since only a certain range of the first four harmonics and the first four sub-harmonics are considered in the proposed PSD model, their summation is less than the total energy of the PSD curve (as demonstrated in the last column of Table 2). The factor β is therefore introduced to balance the total energy of the proposed PSD model and that of the real sample, which is defined as

$$\beta = \frac{S_0}{\sum_{n=0.5}^{4} S_n} \tag{8}$$

where S_0 is calculated by Eq. (7), which is obtained with the same method as S_n in Eq. (7).

Finally, the whole PSD $G(f)$ can be obtained from the superposition of $G_n(f)$ of all the harmonics

$$G(f)=\sum_{n=0.5}^{4}G_n(f) \tag{9}$$

Structure response prediction using the power spectral density model

Root-mean-square response

With the proposed PSD models $G(f)$ of walking load, the root-mean-square (RMS) and the peak acceleration of a floor or footbridge under single pedestrian walking load can be evaluated using stochastic vibration theory (Wirsching and Paez 2006).

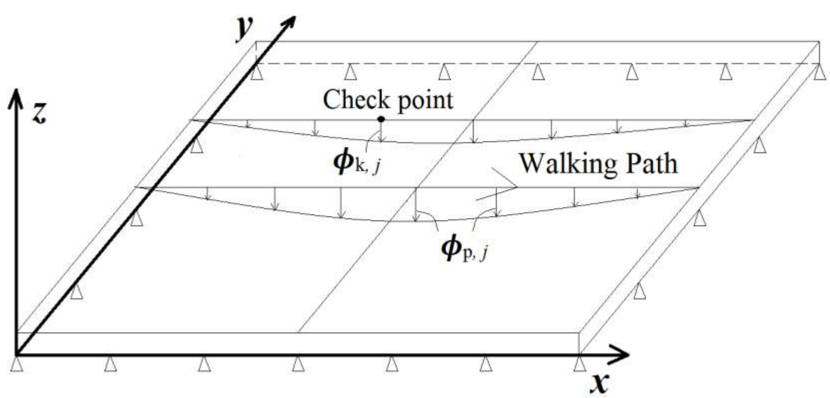

Fig. 7. Walking path on a structure

Suppose that a pedestrian walks across a floor along a path as illustrated in Fig. 7, the induced acceleration at a specified location (hereafter termed as check point) is to be calculated. By the mode-superposition method (Chopra 2005), the linear equation of motion of the *j*th mode of the floor can be expressed as

$$\frac{1}{W}\left(M_j\ddot{q}_j+2\xi_j\omega_jM_j\dot{q}_j+\omega_j^2q_jM_j\right)=\phi_{p,j}(t)\,x_{\mathrm{w}}(t),\qquad (j=1,2,\cdots,m) \tag{10}$$

where q_j, $\dot{q}_j$, $\ddot{q}_j$ are, respectively, the modal displacement, velocity and acceleration, M_j is the modal mass, ξ_j is the damping ratio, ω_j denotes the natural circular frequency of vibration of the *j*th mode, W is the pedestrian's body weight, $x_{\mathrm{w}}(t)$ is the walking load normalized with the body weight W, m is the total number of vibration modes considered for the floor, $\phi_{p,j}(t)$ is the mode shape value at the step point of the pedestrian on the floor at time instant t.

Unlike a jumping load that usually remains on a fixed location, the walking load changes in a temporal-spatial manner. The right side of Eq.(10), i.e., the modal force, is non-stationary, though the walking load $x_{\mathrm{w}}(t)$ is stationary, because $\phi_{p,j}(t)$ changes with time. To deal with this problem, the spectral representation method with amplitude and frequency modulation proposed by Deodatis (1996) is adopted which has been commonly used for seismic response simulation.

Modal force of the *j*th mode can be written as

$$z_j(t) = \phi_{p,j}(t)\, x_{\mathrm{w}}(t) \tag{11}$$

where $x_{\mathrm{w}}(t)$ is the stationary stochastic process and the amplitude modulating function $\phi_{p,j}(t)$ is not related to frequency, but only to time.

To start with, the evolution cross PSD $G_{Z,j,l}(f)$ of the *j*th and the *l*th modal forces, $z_j(t)$ and $z_l(t)$, can be derived from the PSD of $x_{\mathrm{w}}(t)$ (Deodatis 1996), giving

$$G_{Z,j,l}(t,f) = \phi_{p,j}(t)\,\phi_{p,l}(t)\,G(f) \tag{12}$$

Moreover, when the energy distribution is relaxed along with time, e.g. taking its average over time, the evolution PSD of the non-stationary process can be reduced to PSD of a stationary process as an average of time integral (Liang et al. 2007)

$$G_{Z,j,l}(f) = \frac{1}{T_z}\int_{-\infty}^{\infty} G_{Z,j,l}(t,f)\,\mathrm{d}t = G(f)\frac{1}{T_z}\int_{-\infty}^{\infty} \phi_{p,j}(t)\,\phi_{p,l}(t)\,\mathrm{d}t \tag{13}$$

where T_z is the effective duration of the load $z(t)$.

When there are totally N_p steps on the structure, Eq. (13) can be rewritten in a discrete form as:

$$G_{Z,j,l}(f)=\left(\sum_{p=1}^{N_\mathrm{p}}\phi_{p,j}\phi_{p,l}/N_\mathrm{p}\right)G(f) \tag{14}$$

where $\phi_{p,j}$ is the jth mode shape value at pth step point.

According to the mode superposition method, the single-sided PSD $G_R(f)$ of the acceleration at the check point will be:

$$G_R(f)=\sum_{j=1}^{m}\sum_{l=1}^{m}\phi_{\mathrm{k},j}\phi_{\mathrm{k},l}W^2H_j^*(f)H_l(f)G_{Z,j,l}(f) \tag{15}$$

where $\phi_{\mathrm{k},j}$ is the jth mode shape value at the check point (denoted by subscript k), $H_j(f)$ is known as the complex frequency-response function of acceleration and the asterisk denotes a complex conjugate

$$H_j(f)=\frac{-f^2}{M_j\left(-f^2+f_j^2+2i\xi_j f f_j\right)} \tag{16}$$

where f_j is the jth mode's cyclic frequency of the structure, i is the unit imaginary quantity.

Putting Eqs.(10)-(16) together gives $G_R(f)$, and RMS of acceleration α_{rms} is

$$\alpha_{\mathrm{rms}}^2=\int_0^{+\infty}G_R(f)\,\mathrm{d}f \tag{17}$$

Peak response

Peak acceleration is deduced by a peak factor η

$$\alpha_{\mathrm{peak}}=\eta\alpha_{\mathrm{rms}} \tag{18}$$

The peak factor suggested by Vanmarcke (1975) is recommended, which can be used for narrowband random process. The cumulative probability distribution $P(\eta)$ of peak factor η is defined as

$$P(\eta)=\left[1-\exp\left(-\frac{\eta^2}{2}\right)\right]\exp\left[-\nu\bar{T}\frac{1-\exp\left(-\sqrt{\frac{\pi}{2}}\delta^{1.2}\eta\right)}{\exp\left(\frac{\eta^2}{2}\right)-1}\right] \tag{19}$$

where ν is a parameter defined as

$$\nu=2\left(\frac{m_2}{m_0}\right)^{\frac{1}{2}} \tag{20}$$

δ is the bandwidth coefficient defined as

$$\delta=\sqrt{\frac{m_0m_2-m_1^2}{m_0m_2}} \tag{21}$$

$$m_h=\int_0^{+\infty} f^h G_R(f)\, df \tag{22}$$

where $\bar{T}$ is the duration of steady response of structure, and m_h is the hth spectrum moment of the stationary stochastic process.

For a given guarantee probability q, the corresponding peak factor η can be obtained by

$$P(\eta)=q \tag{23}$$

Two values as q = 75% and q = 50% were used in this study to determine η.

Verification of the proposed PSD model

Guided walking case

Figure 8 compares the proposed PSDs of f_p = 1.5, 1.65, 2.0, and 2.25 Hz calculated from Eq. (6)-(9) with those from experiments. It is demonstrated that the proposed PSD model fits well with the experimental samples. The observation is the same for other test cases with prompted walking frequencies.

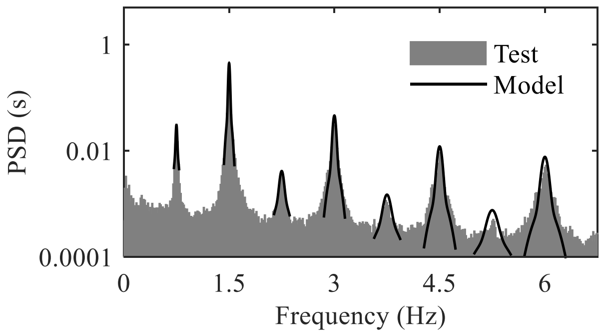

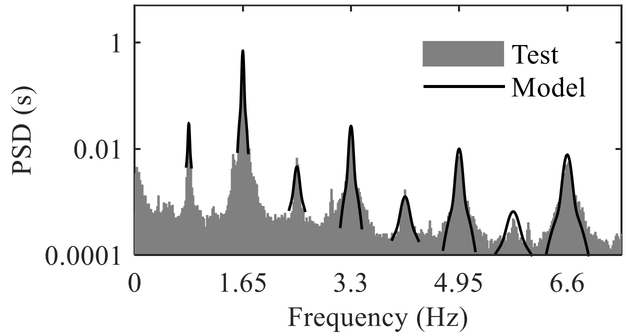

(a) f_p = 1.50 Hz (b) f_p = 1.65 Hz

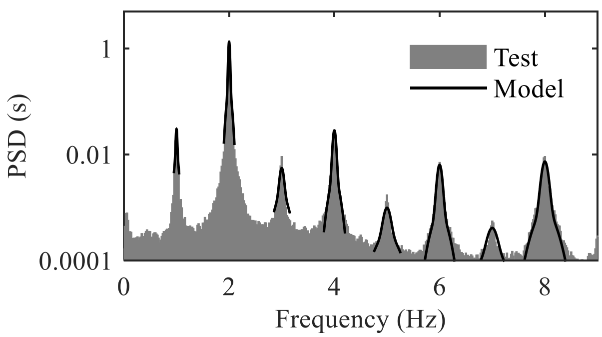

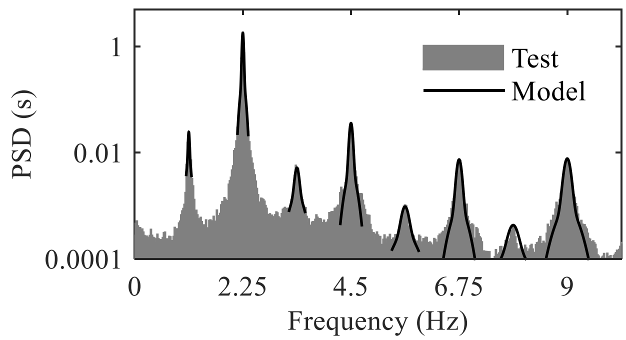

(c) f_p =2.00 Hz (d) f_p = 2.25 Hz

Fig. 8. Comparison of calculated and experimental PSD curves (y axis in logarithmic scale, normalized to weight)

Free-walking case

Experimental records in the free-walking tests were not utilized in developing the PSD model and they were therefore adopted to validate the proposed PSD model. For each record, its experimental PSD was compared with the corresponding theoretical PSD, which was obtained through Eqs. (4)-(7) assuming f_p equals the dominant frequency of the record. Figure 9 shows results of two examples (f_p=1.70 and 2.03 Hz respectively). For both cases, the total spectral energy calculated by the proposed PSD model is in good agreement with the experimental value; the difference is only 0.7% and 0.3% for f_p=1.70 and 2.03 Hz in terms of total energy, respectively. The results for other test cases are similar.

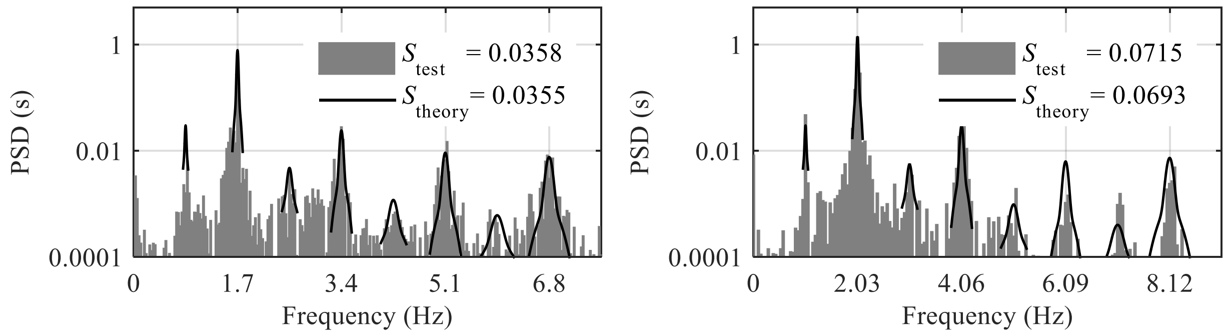

(a) f_p = 1.70 Hz (b) f_p = 2.03 Hz

Fig. 9. Theoretical and experimental PSD of free-walking cases (y axis in logarithmic scale, normalized to weight)

Experiments on floor model

This section compares theoretical response prediction with experimental measurements. To this end, a 10 m × 6 m rectangular concrete floor model was constructed in a lab. The model floor had cast-in-place concrete of grade C40 (characteristic value of compressive strength f_{ck} = 26.8 N/mm^2 and modulus of elasticity E_c = 3.25 × 10^4 N/mm^2) (National Standard of the People's Republic of China 2010) and a thickness of 110 mm. It was simply supported at two ends of the long span (see Fig. 10a).

(a) Tested floor model (b) Individual walking test (c) Walking path and check point

Fig. 10. Experimental setup for the floor model

Fifteen accelerometers (type: Lance LC0132T) were installed beneath the floor to record its responses at various locations including the floor center whose sampling frequency is 200 Hz. The modal properties of the floor were obtained by hammer test. The natural frequencies of the first four vertical vibration modes are 3.48, 6.14, 6.74, and 14.12 Hz, the corresponding modal masses are 8583, 2587, 9625, and 2423 kg, and the damping ratios are 0.02 for all modes.

As demonstrated in Fig. 10b, a test subject weight 813 N was asked to walk along an oval path (see Fig. 10c) at different walking frequencies guided by a metronome. The steady state acceleration measurement at the floor center for 1.75 Hz walking frequency is illustrated in Figure 11. The test results, including RMS for the whole period, peak acceleration and corresponding peak factor, at the floor center for the test cases at resonant frequency (f_p = 1.75 Hz) and three normal walking frequencies (f_p = 1.5, 2 and 2.25 Hz) are summarized in Table 5. The PSD for test response shown in Fig. 12 is obtained via Eq. (1)-(3).

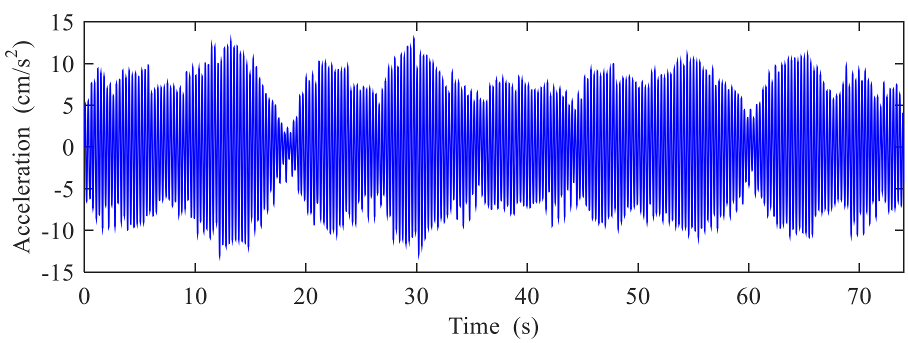

Fig. 11. Measured acceleration of steady state from the test at f_p = 1.75 Hz

The theoretical prediction by spectral model was obtained by the following procedures. First, for a walking frequency f_p in the field test, the corresponding PSD $G(f)$ was obtained from Eqs. (6)-(8). Second, the evolution cross PSD $G_{Z,j,l}(f)$ of modal forces was determined by Eq. (14) where the mode shape values were extracted from a finite element model (mode shapes are shown in Fig. 12). The first four vertical vibration frequencies of the FE model were 3.52, 6.16, 8.97, and 13.19 Hz showing a good match with the measured values. Third, via Eq. (15), the PSD $G_R(f)$ of acceleration at the check point (center of the floor, as shown in Fig. 10c and Fig. 12) was obtained. Finally, RMS was derived from Eq. (17) and peak acceleration with $P(\eta) = 0.5$ and $P(\eta) = 0.75$ from Eqs. (18)-(22). The predicted results of RMS, peak acceleration and peak factor of the proposed model at f_p = 1.5, 1.75, 2, and 2.2 Hz are summarized in Table 5.

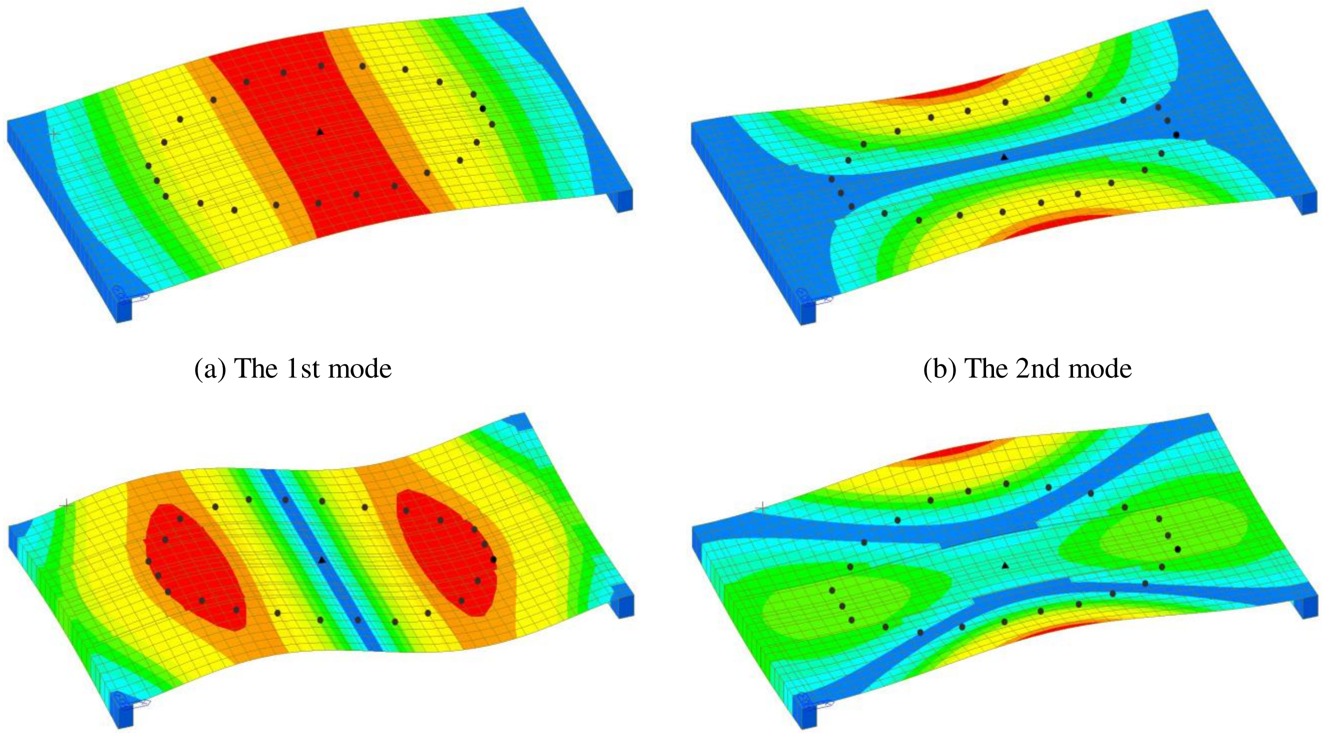

(a) The 1st mode (b) The 2nd mode

(c) The 3rd mode (d) The 4th mode

Fig. 12. Mode shapes of FE model of the floor with the step points (●) and the check point (▲)

Note from Table 5 that the predicted RMS response at resonance frequency (1.75Hz) is about 9% larger than the measured value. For other three walking frequencies, the predicted RMS responses are close to the measured ones with a maximum underestimation of about 20% at 2.2 Hz case. As for peak response, the predicted values for P = 0.5 and P = 0.75 are all larger than the experimental values with only one exception at 2.2 Hz case. The comparison also shows that P = 0.75 will overestimate the structure's peak response especially for resonance situation. Since the floor vibration serviceability problem is not a safety issue in most cases, a guarantee probability P = 0.5 is recommended to predict floor response using the proposed PSD model. Figure 13 further compares the predicted PSD $G_R(f)$ of response around the resonant frequency at f_p = 1.75 Hz with the experimental counterpart, illustrating that they are similar in shape, and the total energies of the two PSDs are close.

Table 5. Comparison between acceleration response at floor center between field test and theoretical prediction

f_p (Hz)	Dur. (s)	Experimental			Theoretical				
						P = 50%		P = 75%	
		α_{rms} (cm/s^2)	α_{peak} (cm/s^2)	η (-)	α_{rms} (cm/s^2)	α_{peak} (cm/s^2)	η (-)	α_{peak} (cm/s^2)	η (-)
1.50	82	1.11	4.97	4.46	1.61	5.59	3.48	6.01	3.74
1.75	84	5.83	13.00	2.23	6.38	19.00	2.98	20.98	3.29
2.00	45	1.95	5.26	2.70	1.84	6.26	3.40	6.74	3.66
2.20	34	2.98	7.95	2.67	2.34	7.89	3.37	8.50	3.63

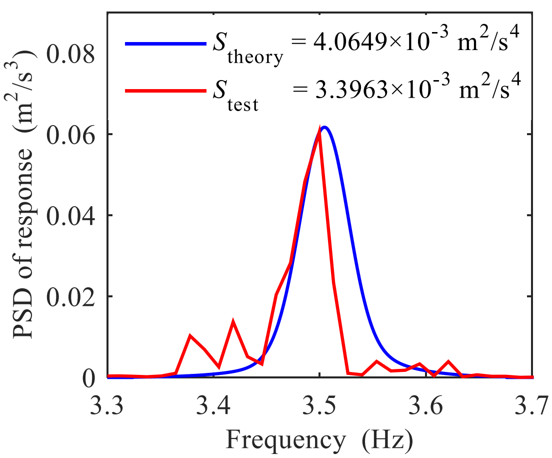

Fig. 13. Theoretical and experimental PSD of response at f_p = 1.75 Hz

Field measurements of an as-built long-span floor

Field measurements of a long-span concrete floor in a railway station in China is used to validate the suggested PSD model. The floor serves as a waiting hall and it has a very long span of 30 m (Fig.14a). The floor has a special structural form composed of a concrete plate and external prestressing tendons underneath the plate (Figs 14b, 14c). The fundamental frequency of the floor was tested as 2.2 Hz and the damping ratio 0.03. Individual walking tests were conducted on this floor and the floor's responses were recorded by accelerometers installed on eight test points (Fig. 14b). The sampling frequency was set as 200 Hz. Figure 15 shows measured accelerations at the floor center from two test cases where the same test subject weight 813 N was asked to walk across the floor along the path shown in Fig. 14b at a frequency of 2.3 Hz twice. More details about the floor and field measurement can be found in Chen et al. (2016).

(a) The floor in use

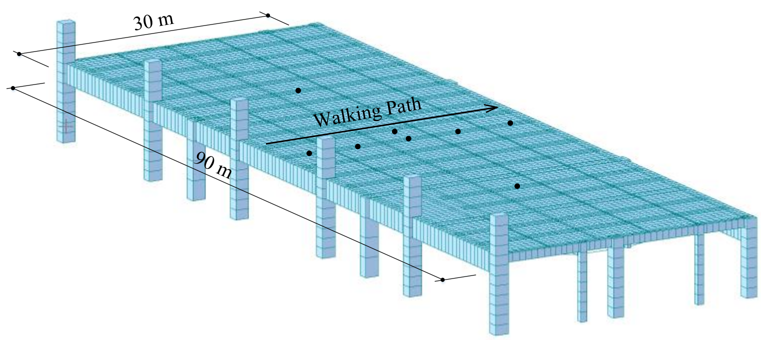

(b) Finite element model with walking path and test points (●)

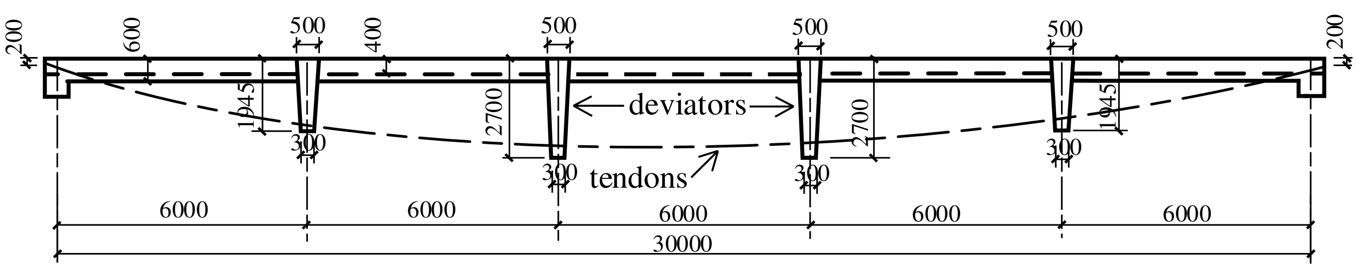

(c) Side view of the floor system (unit: mm)

Fig. 14. The long-span floor in a railway station in China

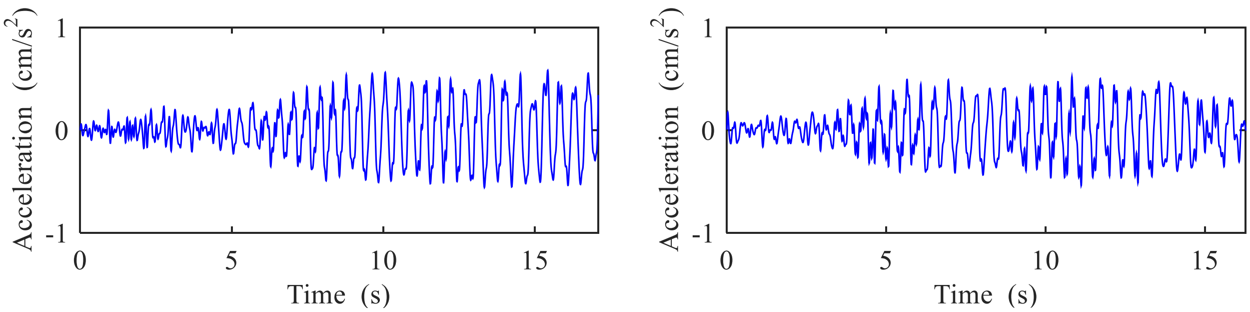

(a) Test case 1 (b) Test case 2

Fig. 15. Measured acceleration at floor center at f_p = 2.3 Hz

For verification purpose, RMS acceleration response at the center of the floor has been predicted by the proposed PSD model with computational parameters given in Table 6. The predicted RMS value calculated from the procedure proposed in this paper is 0.3305 cm/s^2 whilst the RMS values of the two test cases (Fig. 15) are 0.3323 cm/s^2 and 0.2808 cm/s^2, respectively. The comparison demonstrates that the proposed PSD model can be used to predict floor's response to individual walking load.

Table 6. Natural frequencis and modal masses of the floor in the station

Mode	1	2	3	4	5	6	7	8
f_n (Hz)	2.26	2.67	3.01	3.80	4.52	4.62	4.79	4.80
M_n (× 10^5 kg)	7.425	9.069	7.429	8.115	5.325	5.649	4.504	5.514

Discussion

Since records of the individual walking load on rigid floor were utilized to develop the PSD model, the corresponding structural response prediction framework has one limitation that the human-structure interaction (HSI) effect is not considered and this might be one cause for overrating the structure's response (Van Nimmen et al. 2017, Wang et al. 2017). Yet, in most researches relevant to HSI, load models put forward by experiments on a rigid floor are used as portion of contact forces (Van Nimmen et al. 2017), indicating that when the HSI is studied in frequency domain, the proposed PSD load model can be adopted.

In practical design, most codes provide comfort criteria in terms of maximum acceleration or RMS limits with regard to resonant structural response induced by a single pedestrian (ISO 2007, BSI 2003). With the assistance of this proposed PSD model, it is not difficult to estimate the response. A further development of the present work is to model crowd load. To obtain the structural response due to crowd walking, a similar method in this paper can be used, but only with the prerequisite of knowing PSD for crowd load $\mathbf{G}(\mathbf{f})$ presented in matrix as

$$\mathbf{G}(\mathbf{f})=\begin{bmatrix} W_1W_1G_{11}(f) & \cdots & W_1W_uG_{1u}(f) & \cdots & W_1W_{N_\mathrm{h}}G_{1N_\mathrm{h}}(f) \\ \vdots & \ddots & \vdots & \ddots & \vdots \\ W_sW_1G_{s1}(f) & \cdots & W_sW_uG_{su}(f) & \cdots & W_sW_{N_\mathrm{h}}G_{sN_\mathrm{h}}(f) \\ \vdots & \ddots & \vdots & \ddots & \vdots \\ W_{N_\mathrm{h}}W_1G_{N_\mathrm{h}1}(f) & \cdots & W_{N_\mathrm{h}}W_uG_{N_\mathrm{h}u}(f) & \cdots & W_{N_\mathrm{h}}W_{N_\mathrm{h}}G_{N_\mathrm{h}N_\mathrm{h}}(f) \end{bmatrix} \tag{24}$$

where $G_{su}(f)$ is the cross power spectral density between the sth and uth pedestrians. In the matrix, the diagonal elements are just the auto-PSD for each pedestrian proposed in this paper, while the off-diagonal elements $G_{su}(f)$ ($s \neq u$) are undetermined and serve as the kernel of crowd loading problem. To cope with this, a synchronization factor γ is introduced (Wirsching and Paez 2006)

$$G_{su}(f)=\gamma\sqrt{G_s(f)G_u(f)}\,. \tag{25}$$

For two perfectly correlated loads, the synchronization factor $\gamma=1$, while for completely uncorrelated ones, the synchronization factor $\gamma=0$. However, a more realistic situation is that the pedestrian loads present a limited correlation (i.e., $0<\gamma<1$), so evaluating the synchronization factor would be the primary task in subsequent research.

Conclusions

This study proposes a power spectral density model for individual walking load based on statistical analysis of a great number of experimental records, employing a larger database compared with previous walking models in frequency domain. Accounting for the fact that people cannot maintain identical load at each walking step, the new model treats walking load as a random process rather than a perfectly periodic process typically assumed in the majority of existing models. The suggested model describes the spectral amplitudes around a certain range of the first four harmonic and first four sub-harmonic by summation of two Gaussian functions, one accounts for the energy concentration degree and the other accounts for the energy distribution degree of each harmonic or sub-harmonic. The model is expressed in a non-dimensional form similar to that for wind gust load. Model parameters are identified from the experimental data. The proposed spectral density model and its application for predicting structure's acceleration responses by stochastic vibration theory are finally verified by comparing its predictions with measured values from an experimental floor model and an as-built floor.

Acknowledgements

The authors would like to acknowledge the financial support provided by National Natural Science Foundation of China (51778465) and State Key Laboratory for Disaster Reduction of Civil Engineering (SLDRCE14-B-16). Moreover, the authors would like to thank all test subjects for participating in the project making possible the data collection.

Supplemental materials

Experimental dataset of walking load samples in Matlab format is available online in the ASCE Library (ascelibrary.org).

References

Allen, D. E., and Murray, T. M. (1993). "Design criterion for vibrations due to walking." *Engineering Journal,* 30(4), 117-129.

Bachmann, H., and Ammann, W. (1987). "Vibrations in structures: induced by man and machines."

Structural Engineering Documents 3e, International Association for Bridge and Structural Engineering (IABSE), Zurich, Switzerland.

Bendat, J. S, and Piersol, A. G. (2000).*Random Data Analysis and Measurement Procedures*. New York: Wiley & Sons.

Blanchard, J., Davies, B. L., and Smith, J. W. (1997). “Design criteria and analysis for dynamic loading of footbridges.” *Proceedings of the DOE and DOT TRRL Symposium on Dynamic Behaviour of Bridges*, 90-106.

Brownjohn, J. M. W., Pavic, A., and Omenzetter, P. (2004). “A spectral density approach for modelling continuous vertical forces on pedestrian structures due to walking.” *Canadian Journal of Civil Engineering*, 31(1), 65-77.

BSI (British Standards Institution). (2003). “UK National Annex to Eurocode 1: Actions on structures - Part 2: Traffic loads on bridge”. London.

Caprani, C. C. (2014). “Application of the pseudo-excitation method to assessment of walking variability on footbridge vibration.” *Computers & Structures*, 132, 43-54.

Chen, J., Wang, H. Q., and Peng Y. X. (2014). “Experimental investigation on Fourier-series model of walking load and its coefficients.” *Journal of Vibration & Shock*, 33(8), 11-15.

Chen, J., Zhang M. S., and Liu W. (2016). “Vibration serviceability performance of an externally prestressed concrete floor during daily use and under controlled human activities.” *Journal of Performance of Constructed Facilities*, 30(2), 04015007.

Chopra, A. K. (2005). *Dynamics of structures: theory and applications to earthquake engineering*, New Jersey: Prentice Hall.

Dallard, P., Fitzpatrick, A. J., Flint, A., Le Bourva, S., Low, A., Ridsdill Smith, R. M., and Willford, M. (2001). “The London Millennium Footbridge.” *Structural Engineer*, 17–33.

Deodatis, G. (1996). “Non-stationary stochastic vector processes: seismic ground motion applications”. *Probabilistic Engineering Mechanics*, 11(3), 149-168.

Eriksson, P. E. (1994). *Vibration of low-frequency floors: dynamic forces and response prediction.* Ph.D. thesis, Chalmers University of Technology, Goteborg, Sweden.

Ferrarotti, A., and Tubino, F. (2016). “Generalized Equivalent Spectral Model for Serviceability Analysis of Footbridges.” *Journal of Bridge Engineering*, 21(12), 04016091.

Forner Cordero, A., Koopman, H. J. F. M., and van der Helm, F. C. T. (2004). “Use of pressure insoles to calculate the complete ground reaction forces.” *Journal of Biomechanics*, 37, 1427-1432.

Grandke, T. (1983). “Interpolation Algorithms for Discrete Fourier Transforms of Weighted Signals.” *IEEE Transactions on Instrumentation & Measurement*, 32(2), 350-355.

Huang, G. Q., Zheng, H. T., Xu, Y. L., and Li, Y. L. (2015). “Spectrum models for nonstationary extreme winds.” *Journal of Structural Engineering,* 141(10), 04015010.

Haselton, C. B., Baker, J. W., Liel, A. B., & Deierlein, G. G. (2011). “Accounting for ground-motion spectral shape characteristics in structural collapse assessment through an adjustment for epsilon.” *Journal of Structural Engineering,* 137(3), 332-344.

ISO (International Organization for Standardization). (2007). “Bases for Design of Structure — Serviceability of Buildings and Walkways against Vibrations”. ISO 10137, Geneva.

Kerr, S. C. (1998). “Human induced loading on staircases.” Ph.D. thesis, Mechanical Engineering Department, University College London, UK.

Krenk S. (2012). Dynamic response to pedestrian loads with statistical frequency distribution. *Journal of Engineering Mechanics,* 138(10), 1275-1281.

Lee, Y. H., and Hong, W. H. (2005). “Effects of shoe inserts and heel height on foot pressure, impact force, and perceived comfort during walking.” *Applied Ergonomics*, 36(3), 355-362.

Li, Q., Fan, J. S., Nie, J. G. et al. (2010). Crowd-induced random vibration of footbridge and vibration control using multiple tuned mass dampers. *Journal of Sound and Vibration,* 329, 4068-4092.

Liang, J., Chaudhuri, S. R., and Shinozuka, M. (2007). “Simulation of Nonstationary Stochastic Processes by Spectral Representation.” *Journal of Engineering Mechanic*, 133(6), 616-627.

National Standard of the People's Republic of China. (2010). “Code for design of concrete structures.” GB50010-2010, China Architecture & Building Press, Beijing.

Ohlsson, S. V. (1982). *Floor Vibration and Human Discomfort*, Ph.D. thesis, Chalmers University of Technology, Goteborg, Sweden.

Petersen, C. (1996). *Dynamik der Baukonstruktionen*, Vierweg, Braunschweig /Wiesbaden (in German).

Piccardo, G., and Tubino, F. (2012). “Equivalent spectral model and maximum dynamic response for the serviceability analysis of footbridges.” *Engineering Structures*, 40, 445-456.

Racic, V., and Brownjohn, J. M. W. (2011). “Stochastic model of near-periodic vertical loads due to humans walking.” *Advanced Engineering Informatics*, 25(2), 259-275.

Racic, V., and Pavic, A. (2010). “Stochastic approach to modelling of near-periodic jumping loads.” *Mechanical Systems & Signal Processing*, 24(8), 3037-3059.

Rainer, J. H., Pernica, G., and Allen, D.E. (1988). “Dynamic loading and response of footbridges.” *Canadian Journal of Civil Engineering*, 15(1), 66-71.

Van Nimmen, K., Lombaert, G., De Roeck, G., and Van den Broeck, P. (2017). “The impact of vertical human-structure interaction on the response of footbridges to pedestrian excitation.” *Journal of Sound & Vibration,* 402, 104-121.

Vanmarcke, E. H. (1975). “On the distribution of the first-passage time for normal stationary random processes.” *Journal of Applied Mechanics*, 42(1), 2130-2135.

Wang, H. Q., Chen, J., and Brownjohn, J. M. W. (2017). “Parameter identification of pedestrian’s spring-mass-damper model by ground reaction force records through a particle filter approach.” *Journal of Sound and Vibration*, 411(22), 409-421.

Welch, P. D. (1967). “The use of fast Fourier transform for the estimation of power spectra: A method based on time averaging over short, modified periodograms.” *IEEE Transactions on Audio & Electroacoustics*, AU-15(2), 70-73.

Wirsching, P. H., Paez, T. L., and Ortiz, K. (2006). *Random Vibrations: Theory and Practice*. New York: Wiley Publication.

Yoneda, M. (2002). “A simplified method to evaluate pedestrian-induced maximum response of cable-supported pedestrian bridges.” *Proceedings of the International Conference on the Design and Dynamic Behaviour of footbridges*. Paris, France.

Živanović, S. (2012). “Benchmark Footbridge for Vibration Serviceability Assessment under Vertical Component of Pedestrian Load.” *Journal of Structural Engineering*, 138(10), 1193-1202.

Živanović, S., Pavić, A., and Reynolds, P. (2007). “Probability-based prediction of multi-mode vibration response to walking excitation.” *Engineering Structures*, 29(6), 942-954.

Živanović, S., and Pavić, A. (2015). “Quantification of dynamic excitation potential of pedestrian population crossing footbridges." *Shock & Vibration*, 18(4), 563-577.

Živanović, S., Pavić, A., and Ingólfsson, E. T. (2010). "Modelling Spatially Unrestricted Pedestrian Traffic on Footbridges." *Journal of Structural Engineering*, 136(10), 1296-1308.

A list of figure captions

Fig.1. Test subject with Pedar insole system in the experiment

Fig. 2. Typical testing samples at f_p = 1.50 Hz (a) Normalized vertical force of left, right foot and their summation (b) Fourier amplitude spectrum of total force

Fig. 3. The PSD of a walking load sample normalized to body weight at f_p = 1.50 Hz (df = 0.0325 Hz) (a) The 1st harmonic (b) The 2nd harmonic (c) The 3rd harmonic (d) The 4th harmonic

Fig. 4. The PSD $G_{X_w}(f)$ of the new samples normalized to body weight with df = f_p /100 (a) f_p = 1.50 Hz (b) f_p = 2.25 Hz

Fig. 5. Superimposed PSD of the new samples and their average (a) The 1st harmonic (b) The 2nd harmonic (c) The 3rd harmonic (d) The 4th harmonic (e) The 1st sub-harmonic (f) The 2nd sub-harmonic (g) The 3rd sub-harmonic (h) The 4th sub-harmonic

Fig. 6. Normalized PSDs of four harmonics (sub-harmonics), the average and the two-term Gaussian fit (a) Harmonic (b) Sub-harmonic

Fig. 7. Walking path on a structure

Fig. 8. Comparison of calculated and experimental PSD curves (y axis in logarithmic scale, normalized to weight) (a) f_p = 1.50 Hz (b) f_p = 1.65 Hz (c) f_p =2.00 Hz (d) f_p = 2.25 Hz

Fig. 9. Theoretical and experimental PSD of free-walking cases (y axis in logarithmic scale, normalized to weight) (a) f_p = 1.70 Hz (b) f_p = 2.03 Hz

Fig. 10. Experimental setup for the floor model (a) Tested floor model (b) Individual walking test (c) Walking path and check point

Fig. 11. Measured acceleration of steady state from the test at f_p = 1.75 Hz

Fig. 12. Mode shapes of FE model of the floor with the step points (●) and the check point (▲) (a) The 1st mode (b) The 2nd mode (c) The 3rd mode (d) The 4th mode

Fig. 13. Theoretical and experimental PSD of response at f_p = 1.75 Hz

Fig. 14. The long-span floor in a railway station in China (a) The floor in use (b) Finite element model with walking path and test points (●) (c) Side view of the floor system (unit: mm)

Fig. 15. Measured acceleration at floor center at f_p = 2.3 Hz (a) Test case 1 (b) Test case 2